International Journal of Energy and Environmental Engineering
ISSN: 2008-9163
Vol.2 / No.2 (pp.65-75) / Spring 2011

Numerical Investigation of Tub Side Heat Transfer and Pressure Drop in Helically Corrugated Tubes

S. Hossainpour[*1] and R. Hassanzadeh[2]

[1]Department of Mechanical Engineering, Sahand University of Technology, Tabriz 51325-1996, Iran
[2]Department of Mechanical Engineering, Islamic Azad University Tabriz Branch, Iran

Received Date: 15 Jan.; 2011 Accepted: 25 Apr.; 2011

ABSTRACT

This paper presents a three-dimensional numerical investigation carried out in turbulent forced convection in a tube with helical ribs. Enhancement of heat transfer using helically corrugated tubes has been studied experimentally by many researchers but there exist a few published numerical analyses results. The paper also introduces the results of heat transfer and friction factor data for incompressible fluid flow in a tube with 24 mm inside diameter and Reynolds numbers between 25000-80000. The geometric parameters of single start internally ribbed tubes are, rib height to diameter ratio ranging from 0.02 to 0.06 and rib pitch to diameter ratio ranging from 0.6 to 1.2. The inlet water temperature is 10^{o}C and tube wall is at 80^{o}C uniform temperature. Tube side, three-dimensional turbulent flow has been simulated using a finite volume code and the results are compared with available experimental data. It has been shown that the helical ribs have a significant effect on the heat transfer augmentation and pressure drop.

Keywords

Heat transfer enhancement, helical rib, corrugated tube, friction factor, turbulent flow

1. Introduction

The improvement of convective heat transfer in thermal systems is needed in many engineering applications in conjunction with reducing the size, weight and cost of heat exchanger equipment. In general, the heat transfer enhancement techniques can be divided into two groups (active and passive techniques). Tubes with helical rib are one of the passive techniques for heat transfer enhancement, and are the most widely used tubes in several heat transfer applications, such as air conditioning and refrigeration, chemical process and recovery systems [1]. Spirally corrugated tubes have become important in commercial applications for turbulent single phase flow due to 1- The pressure drop increment is generally compensated by the heat transfer augmentation. 2- The amount of tube material used in the tube manufacturing neither increases nor decreases. 3- Manufacturing process is easy and cheap [2]. The prospect of using the helically corrugated tube is for reducing the thickness of the boundary layer or thinning of the boundary layer which is aimed at better fluid mixing near the tube wall caused by the secondary flows from the wall to the core flow. Corrugated tubes have been widely studied during the last 35 years. Vicente et al. compared spirally-corrugated tube correlations of 8 different researchers and concluded that for the same operating conditions differences in prediction of friction factors and Nusselt numbers can be as high as 231 and 167 percent, respectively [2]. Vicente et al. performed experiments on a family of 10 helically corrugated tubes under the following conditions: non-dimensional height ranging

[*] Corresponding author: S.Hossainpour (e-mail: hossainpour@sut.ac.ir)
Tel: +98-412-3459067; fax: +98-412-3444309

from 0.02 to 0.06, non-dimensional pitch from 0.6 to 1.2, Reynolds numbers from 2000 to 90000, and Prandtl Number from 2.5 to 100. Ravigururajan and Bergles [3] used turbulent water flow in a transparent plexiglass tube with a wire coil insert and proposed general correlations for prediction of heat transfer coefficient and friction factor. The work of Li et al. [4] was the first study that attempted to describe the mechanisms of heat transfer in helically-finned tubes with visualization. Li et al., limited their analysis to single-start tubes because, based on their flow visualizations, single-start tubes achieve higher intensities of boundary layer separation than multiple-start tubes with the same parameters. Thus, according to Li et al., single-start tubes are more beneficial for heat transfer applications. Nakayama et al. [5] tested tubes with spiral ribs having helix angles ranging from 0^o to 80^o and between 2 and 10 starts. Jensen and Vlakancic tested fifteen helically-finned tubes with a wide rang of helix angles (0^o-45^o), e/D ratios (0.0075-0.085), number of starts (8-45), and fin widths (0.62 mm -1.84 mm) [5]. An earlier study conducted by Gee and Webb investigated tubes with helical square-shaped ribs. The helix angle varied between 30^o and 70^o, and the pitch was held constant at 3.81 mm. They used air at Reynolds numbers varying from 6000 to 65000 [6]. Mimura and Isozaki [7] studied the effect of the shapes of corrugated tubes with different relative depths and relative pitches on the heat transfer and pressure drop characteristics. The tube side heat transfer coefficient obtained from two start corrugated tubes was slightly smaller than those from single start tubes. Withers [8] tested fourteen single-helix corrugated tubes at various Reynolds and Prandtl numbers ($10000< Re <120000$; $2.3< Pr< 10.4$). A review of measurements of global heat transfer coefficient and pressure drop for various rib configurations (square ribs) was given by Dalle Donne and Meyer [9]. Martin and Bates [10] presented velocity field and the turbulence structure in an asymmetrically ribbed rectangular channel with one rib configuration (square ribs) and varying channel height. Hong and Hsieh [11] investigated the influence of rib alignment on forced convection in a channel at different rib alignments, either staggered or in-line, on the internal surfaces of rectangular or square channels. Jaurker et al. [12] reported the heat transfer and friction characteristics of rib grooved artificial roughness on one broad heated wall of a large aspect ratio duct. Numerical investigations on turbulent flow friction and heat transfer enhancement in ducts or channels with rib, groove or rib–groove turbulators have been carried out extensively. Chaube et al. investigated the flow and heat transfer characteristics of a two dimensional rib roughened (rectangular/chamfered rib) rectangular duct with only one principal heating wall by using the shear stress transport k–ω turbulence model [13]. Saidi and Sunden studied the thermal characteristics in a duct with rib turbulators using a simple eddy viscosity model and an explicit algebraic stress model and reported that the algebraic stress model has some superiority over the eddy viscosity model for only velocity field structure prediction [14]. Tatsumi et al. investigated numerically the flow around a discrete rib attached obliquely to the flow direction onto the bottom wall of a square duct and found that noticeable heat transfer augmentation was obtained downstream of the rib, produced by a strong secondary flow motion [15]. Yang and Hwang numerically examined the heat transfer enhancement in rectangular ducts with slit and solid ribs mounted on one wall using the k–ε turbulence model [16]. Luo et al. reported the turbulent convection behavior in a horizontal parallel-plate channel with periodic transverse ribs using the standard k–ε model and a Reynolds stress model [17]. Based on the literature survey, there are few publications that present numerical solutions of laminar or turbulent flow in helically ribbed tubes [5]. Numerical solutions of turbulent flows are complex because turbulent fluid flow in helically ribbed tubes is difficult to model and few attempts have been made to obtain numerical solutions. So, this study has been conducted to investigate numerically the flow characteristics in tubes with helical ribs.

2. Mathematical model

Due to boundary layer displacement and existing of rotational layer, turbulent fluid flow behavior in corrugated tubes with helical ribs is complex. Some experimental attempts have been

done for realization of flow behavior in these tubes. Ravigururajan and Bergles drew the following conclusions from the photographs [5].

1. Flow visualization tests indicated the presence of a rotational layer close to the wall and a crossover layer in the core of the tube. The rotational pattern dominated for helix angles less than 30°and the crossover pattern dominated for helix angles larger than 70°.
2. As the roughness height increased, the angle of fluid rotation was increased.
3. Deceasing the helix angle decreased turbulence and the transition Re.
4. The thickness of the rotational layer decreased with increasing Re.
5. Rotational angles tended towards the helix angle as Re was decreased.

Photographs taken by Li et al. showed that spiral flow and boundary layer separation both occurred in helical ribbed tubes, but with different intensities in tubes having different configurations [4]. Swirl of flow is known to augment heat transfer.

This tends to increase the effective flow length of the fluid through the tube, which increases heat transfer and pressure drop. Boundary layer separation is also known to augment heat transfer. Periodic boundary layer separation causes that turbulence intensity to increase. So Heat transfer rate and pressure drop will be increase. Flow governing equations based on assumptions that flow is incompressible and steady in the Cartesian coordinates are:

Continuity equation

$$\frac{\partial u_i}{\partial x_i} = 0 \tag{1}$$

Momentum equation

$$\rho \frac{\partial}{\partial x_j}(u_i u_j) = -\frac{\partial p}{\partial x_i} + \frac{\partial}{\partial x_j}\left[\mu\left(\frac{\partial u_i}{\partial x_j} + \frac{\partial u_j}{\partial x_i}\right)\right] + \rho \frac{\partial}{\partial x_j}\left(-\overline{u_i' u_j'}\right) \tag{2}$$

Energy equation

$$\rho \frac{\partial}{\partial x_i}(u_i T) = \frac{\partial}{\partial x_j}\left[(\Gamma + \Gamma_t)\frac{\partial T}{\partial x_j}\right] \tag{3}$$

Where Γ and Γ_t are molecular thermal diffusivity and turbulent thermal diffusivity, respectively and are given by:

$$\Gamma = \frac{\mu}{\mathrm{Pr}} \quad \text{and} \quad \Gamma_t = \frac{\mu_t}{\mathrm{Pr}_t} \tag{4}$$

Reynolds stresses are related to the mean velocity gradients using Boussinesq assumption.

$$-\rho\overline{u_i' u_j'} = \mu_t\left(\frac{\partial u_i}{\partial x_j} + \frac{\partial u_j}{\partial x_i}\right) \tag{5}$$

The turbulent viscosity term μ_t is computed from well-known standard k-ε turbulence model. The expression for the turbulent viscosity is given as:

$$\mu_t = \rho C_\mu \frac{k^2}{\varepsilon} \tag{6}$$

Heat transferred to water at constant wall temperature, Q_w, can be calculated from:

$$Q_w = h.A.(T_s - T_{w.ava}) \tag{7}$$

The heat transfer is measured by local Nusselt number, which can be obtained by:

$$Nu = \frac{h.d_H}{\lambda} \tag{8}$$

The friction factor for the tube with helical rib, f_{he}, can be calculated from:

$$f_{he} = \frac{\Delta p}{\left[\left(\rho u^2 / 2\right)\left(L / d_H\right)\right]} \tag{9}$$

Where Δp is pressure drop between inlet and outlet of tube, ρ is density of water, u is average velocity at center line, L is tube length and d_H is hydraulic diameter of the tube.

Nusselt number and friction factor in plain tube can be calculated from Gnielinski correlations [18]:

$$Nu_D = \frac{\left(\frac{f_p}{8}\right)(\mathrm{Re}_D - 1000)\mathrm{Pr}}{1 + 12.7\left(\frac{f_p}{8}\right)^{\frac{1}{2}}\left(\mathrm{Pr}^{\frac{2}{3}} - 1\right)} \tag{10}$$

$$f_p = \left(0.79 \ln . \mathrm{Re}_D - 1.64\right)^{-2} \tag{11}$$

In contrast to the molecular viscosity, the eddy viscosity depends strongly on the flow property. Therefore, selecting the turbulence model, to accomodate the flow behavior of each application, is very important.

The standard k–ε turbulence model is used in this investigation. The steady incompressible Navier–Stokes equations and the turbulence closure equations were solved using the finite volume code.

3. Investigated helical tube geometry

The system of interest is a horizontal tube with helical ribs at two categories. One category is to analyze the effects of rib height on the heat transfer and friction factor at the constant rib pitch and another is to analyze the effects of rib pitch on the heat transfer and friction factor at the constant rib height. Fig. 1 shows a schematic figure of a single-start corrugated tube, where p stands for helical pitch, e for height of the rib, and β for helical angle.

Fig. 2 shows a view of computational mesh used in this investigation and Table. 1 shows details of two cases consisting of 6 models used in this study. A composite mesh such as shown in Fig. 2 is used for all cases to resolve some flow details near ribs. The length of all tubes is 500 mm and the inside diameter of tubes is 24 mm. A finite volume based CFD code that use SIMPLE algorithm for pressure coupling was used to solve governing flow equations with associated boundary conditions.

4. Numerical results

Predicted results are reported for fully developed flow through the tube with helical ribs at Reynolds numbers between 25000-80000. Figures 3-5 show the temperature, total relative pressure and velocity magnitude contour plots for e/D=0.04, p/D=0.6 at Re=52893, respectively. Mesh independency for all of the results were controlled and Table 2 shows the final grid size for each case. In order to clarify mesh independency, one of the cases (e/D=0.06,p/D=0.8) is selected and studied.

Table 3 shows the details of grid refinement results for selected case. The velocity components in second corrugated rib tip is used for this propose. This table shows that our numerical results are grid size independent. The comparison between numerical result of present work and experimental results of Ravigururajan and Bergles [3] shows total agreement between them. Fig. 6 shows sample comparisons for Nusselt number where e/D=0.02, p/D=0.8 and e/D=0.04, p/D=1.2.

Figures 7 and 8 show the variation of Nusselt number with Reynolds number for two categories. As shown in this figures, the heat transfer coefficient increases with increasing Reynolds number. However, this effect tends to deduct as the Reynolds number increases. Fig. 7 also shows the effect of helical rib depth on the Nusselt number in different Reynolds number. It can be clearly seen that the Nusselt number increases with increasing helical rib depth in fix Reynolds numbers.

This is because the helical rib depth has a significant effect on the mixing of the fluid in the boundary layer and increasing the turbulent intensity of fluid flow. In addition, as seen from Fig. 8 flow reattaches on the base wall and then flows up over the next rib.

The reattachment length strongly depends on to helical rib depth. Therefore, the heat transfer coefficient increases with helical rib depth. According to Fig. 9, it can be seen that the heat transfer coefficient tends to increase as the helical rib pitch decreases. The reason for this can be explained similarly as that for the depth mentioned above.

In general, the flow through the tube with helical rib is quite complex. However, the pressure drop across the tube with helical rib is produced by (1) drag forces exerted on the flow field by the helical rib (2) flow blockage due to area reduction (3) turbulence augmentation and (4) rotational flow produced by the helical rib [2]. Figures 10 and 11 show the variation of friction factor with Reynolds number for two categories. According to these figures the friction factor decreases with increasing Reynolds number.

As expected, the friction factor obtained from the tube with higher helical rib depth and lower helical rib pitch are significantly higher than those with lower helical rib depth and higher rib pitch.

5. Conclusion

Numerical analyses on the heat transfer coefficient and friction factor of horizontal tubes with helical ribs are presented. The effects of the heli-

cal ribs configuration on the heat transfer and pressure drop characteristics are also considered. The heat transfer and friction factor augmentations obtained from this study are compared with those from the tube without helical rib (plain tube). At the end, the comparison between numerical data and Ravigururajan and Bergles [3] experimental data showed that there are reasonable agreement between them.

6. Nomenclature

A	area, m^2
C_μ	turbulence model constant
d_H	hydraulics diameter, m
e	helical rib depth, m
f	friction factor
h	heat transfer coefficient, w m^{-2} K^{-1}
k	turbulence energy, m^2 s^{-2}
L	length, m
$\dot{m}$	mass flow rate, kg s^{-1}
Nu	Nusselt number
P	helical rib pitch, m
p	pressure, Pa
Pr	Prandtl number
Re	Reynolds number
T	temperature, ^oC
Q	heat transfer rate, w
U	mean velocity, m s^{-1}
u_i	velocity component in I direction, m/s
u'_i	fluctuation velocity components, m/s
x_i	Cartesian coordinate directions, m

Greek letter

μ	kinematic viscosity, kg s^{-1} m^{-1}
λ	thermal conductivity, w m^{-1} K^{-1}
μ_t	eddy viscosity, kg s^{-1} m^{-1}
ε	turbulent dissipation rate m^2 s^{-3}
ρ	density, kg m^{-3}

Subscripts

ava	average
p	plain tube
s	surface wall
he	helical rib
w	water

References

[1] Webb R. L., Kim N. H. , Principles of Enhanced Heat Transfer, 2nd edition, Taylor & Francis, (2005)

[2] Vicente PG., Garcia A., Viedma A., Experimental investigation on heat transfer and friction factor characteristics of spirally corrugated tubes in turbulent flow at different Prandtl number, Int. J Heat Mass Tran. 47 (2004) 671-81.

[3] Ravigururajan. T.S., and Bergles, A.E., Development and Verification of General Correlations for Heat Transfer and Pressure Drop in Single-Phase Turbulent Flow in Enhanced Tubes, Exp. Therm. Fluid Sci. 13 (1996) 55-70.

[4] Li HM, Ye KS, Tan YK, Deng SJ, Investigation of tube-side flow visualization, friction factor and heat transfer characteristics of helical-ribbing tubes. Proceedings of the 7th heat transfer conference, Washington, Hemisphere Publishing Corp., 1998, pp. 75-80.

[5] Zdaniuk, G., Heat Transfer and Friction Factor in Helically-Finned Tubes using Artificial Neural Networks, Ph.D. thesis, Mississippi State University, Department of Mechanical Engineering, 2006.

[6] Gee D.L., and Webb R.L., Forced convection heat transfer in helically rib-roughened tubes, Int. J. Heat Mass Tran. 23 (1980) 1127-1136.

[7] Mimura K., Isozaki A., Heat transfer and pressure drop of corrugated tubes, Desalination 22, (1977) 131–139.

[8] Withers J.G., Tube-Side Heat Transfer and Pressure Drop for Tubes Having Helical Internal Ridging with Turbulent/Transitional Flow of Single-Phase Fluid. Part 1. Single-Helix Ridging, Heat Transfer Engineering 2 (1) (1980) 48-58.

[9] Dalle Donne M., Meyer L., Turbulent convective heat transfer from rough surfaces with two-dimensional rectangular ribs, Int. J. Heat Mass Tran. 20 (1977) 583–620.

[10] Martin S.R., Bates C.J., Small-probe-volume Laser Doppler Anemometry measurements of turbulent flow near the wall of a rib-roughened channel, Flow Measurement Instrumentation 3 (1992) 81-88.

[11] Hong Y.M., Hsieh S.S., Heat transfer and friction factor measurement in ducts with staggered and in line ribs, Transaction ASME, Journal of Heat Transfer 115 (1993) 58–65.

[12] Jaurker A.R., Saini J.S., Gandhi B.K., Heat transfer and friction characteristics of rectangular solar air heater duct using rib–grooved artificial roughness, Solar Energy 80 (2006) 895–907.

[13] Chaube A., Sahoo P.K., Solanki S.C., Analysis of heat transfer augmentation and flow characteristics due to rib roughness over absorber plate of a solar air heater, Renewable Energy 31 (2006) 317–331.

[14] Saidi A., Sunden B., Numerical simulation of turbulent convective heat transfer in square ribbed ducts, Numerical Heat Transfer, Part A: Applications 38 (1) (2000) 67–88.

[15] Tatsumi K., Iwai H., Inaoka K., Suzuki K., Numerical analysis for heat transfer characteristics of an oblique discrete rib mounted in a square duct, Numerical Heat Transfer, Part A: Applications 44 (8) (2003) 811–831.

[16] Yang Y.T., Hwang C.W., Numerical calculations of heat transfer and friction characteristics in rectangular ducts with slit and solid ribs mounted on one wall, Numerical Heat Transfer, Part A: Applications 45 (4) (2004) 363–375.

[17] Luo D.D., Leung C.W., Chan T.L., Wong W.O., Flow and forced-convection characteristics of turbulent flow through parallel plates with periodic transverse ribs, Numerical Heat Transfer, Part A: Applications 48 (1) (2005) 43–58.

[18] Incropera, F. P., and DeWitt, D. P., 1996, Fundamentals of Heat and Mass Transfer, 4th Ed., John Wiley and Sons, New York.

Table 1. Details of two cases consisting of 6 models used in this study

Case	e/D	p/D	Number of starts	Helix angle
1	0.02 0.04 0.06	0.8	single	75.7 75.7 75.7
2	0.04	0.6 0.8 1.2	single	79 75.7 69

Table 2. Mesh independent grid size for each case

No.	e/D	p/D	Cells No.	Faces No.	Nodes No.
1	0.02	0.8	589384	1351190	221905
2	0.04	0.8	608886	1395686	227880
3	0.06	0.8	752445	1701659	261442
4	0.04	0.6	702480	1620276	273589
5	0.04	1.2	646009	1500868	261129

Table 3. Mesh independency study for e/D=0.06,p/D=0.8

Case	1 (Final mesh)	2 (more refined mesh)
Cells No.	752445	2812587
Faces No.	1701659	5706750
Nodes No.	261442	509468
U m/s	1.2316	1.2455
V m/s	-0.01387	-0.01400

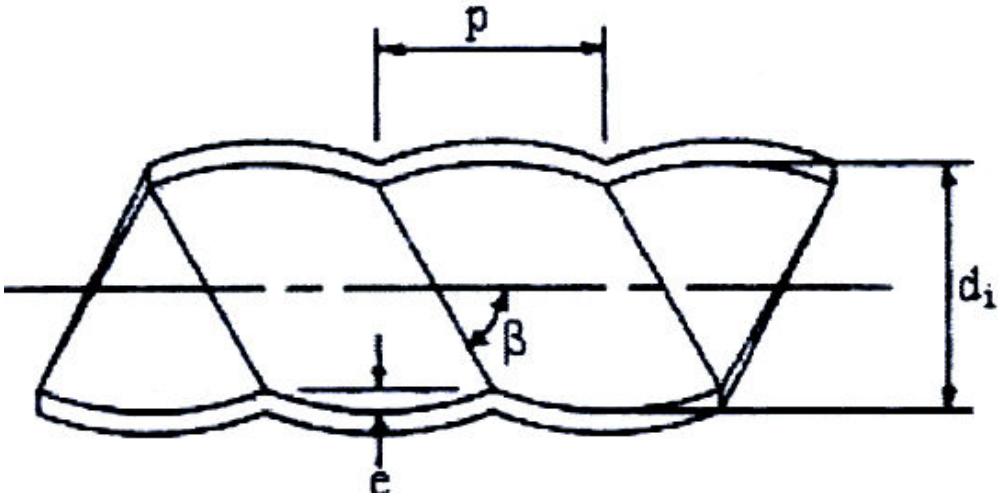

Fig.1: Sketch of a single-start corrugated tube

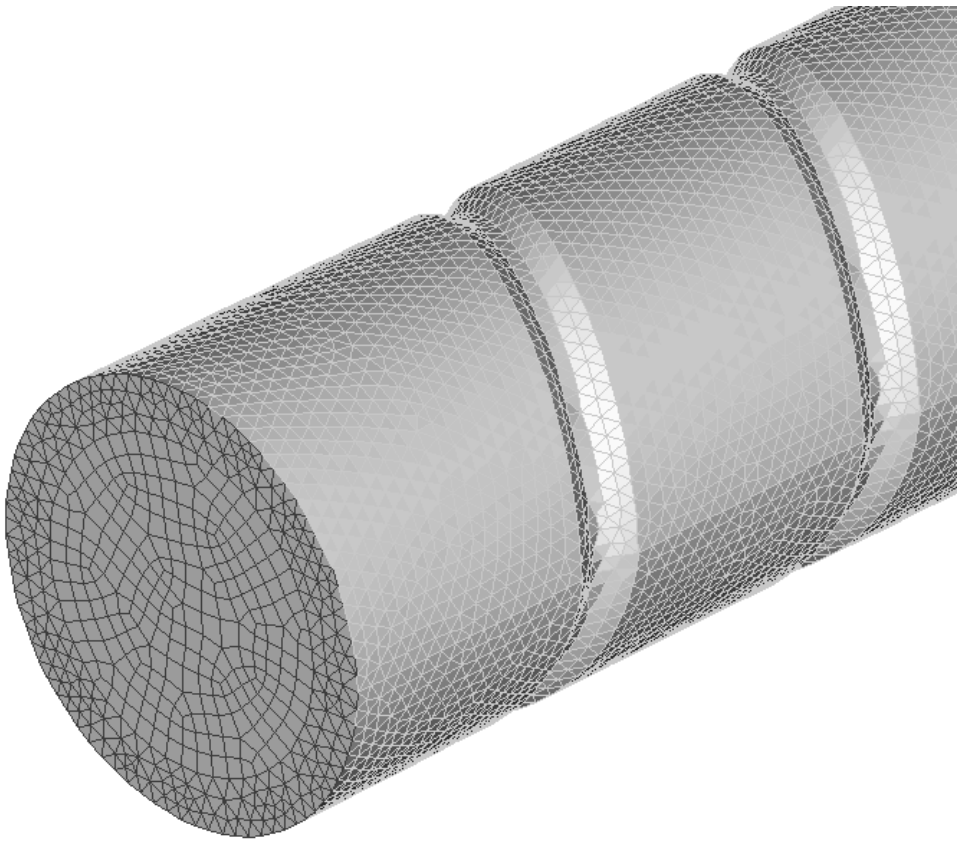

Fig.2: A view of composite grid mesh

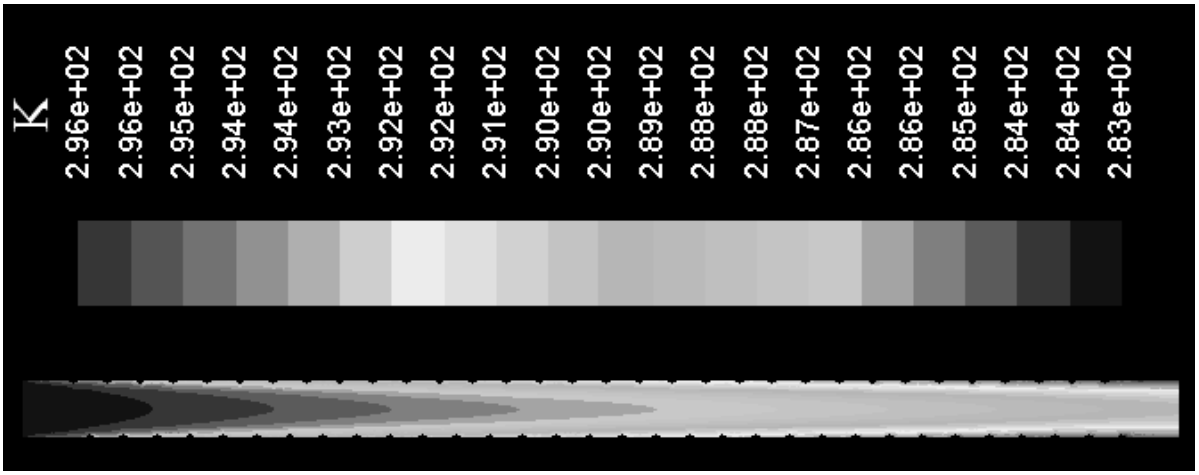

Fig.3: Temperature contour plot for e/D=0.04, p/D=0.6 at Re=52892

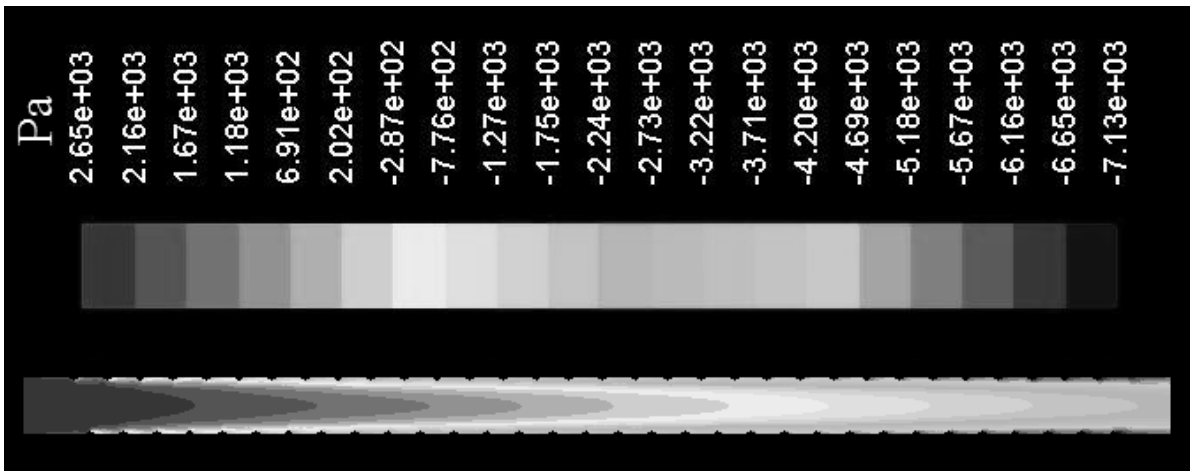

Fig.4: Relative total pressure contour plot for e/D=0.04, p/D=0.6 at Re=52892

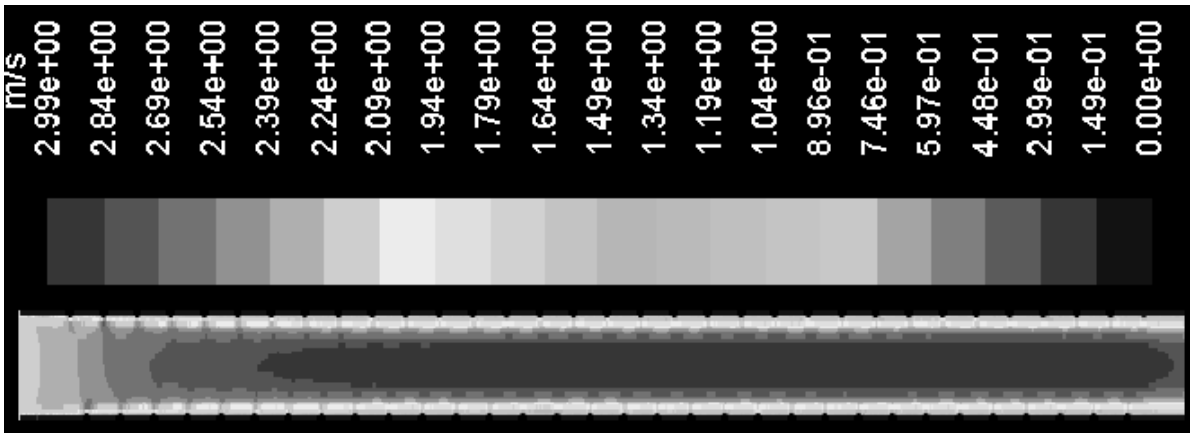

Fig.5: Velocity magnitude contour plot for e/D=0.04, p/D=0.6 at Re=52892

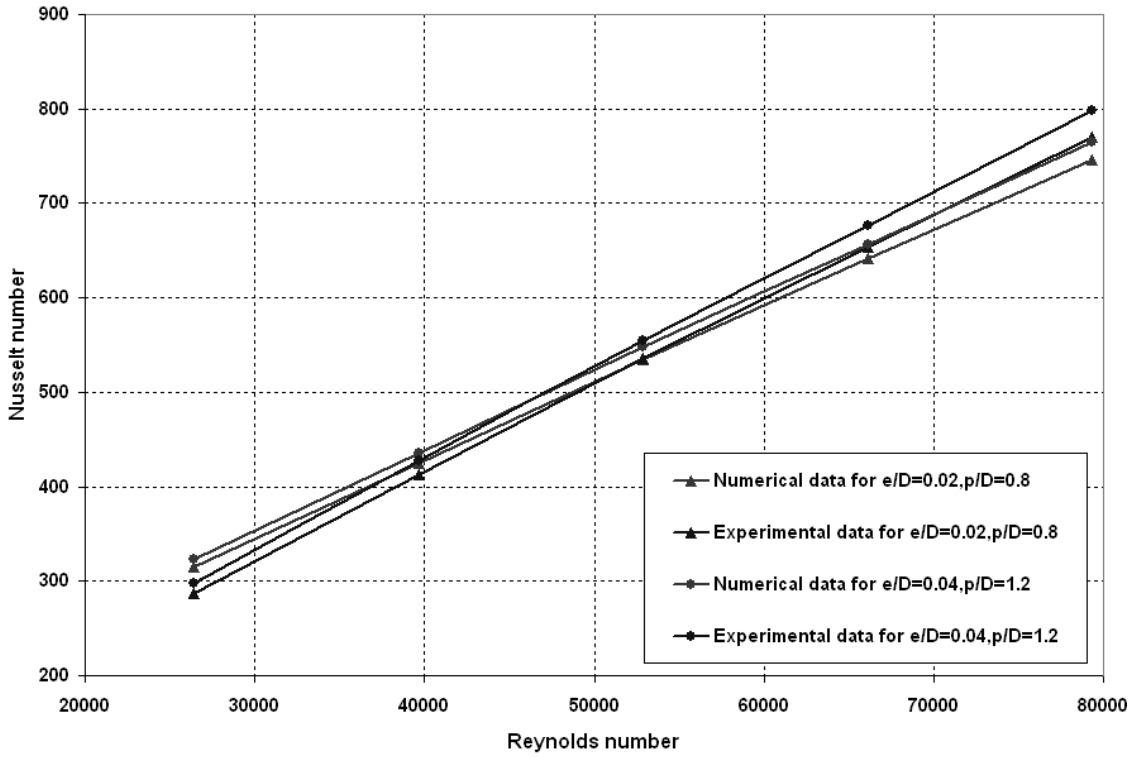

Fig.6: Comparison of calculated Nusselt number and experimental values obtained by Ravigururajan and Bergles [3]

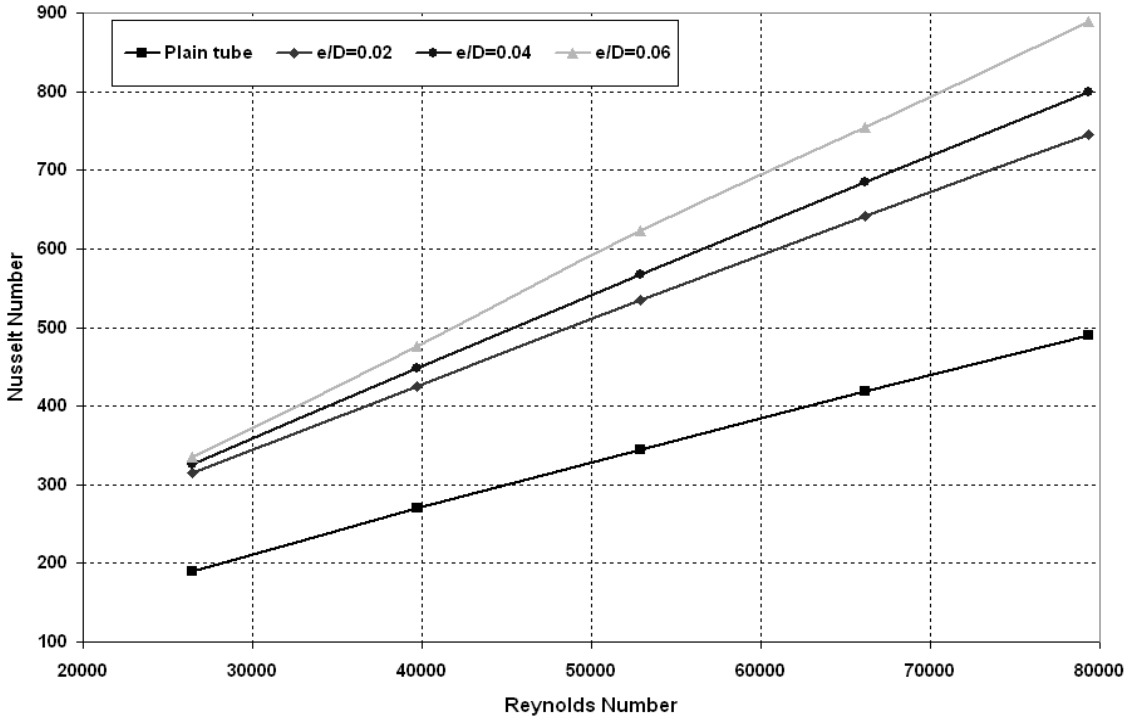

Fig.7: Variation of Nusselt number with Reynolds number for p/D=0.8

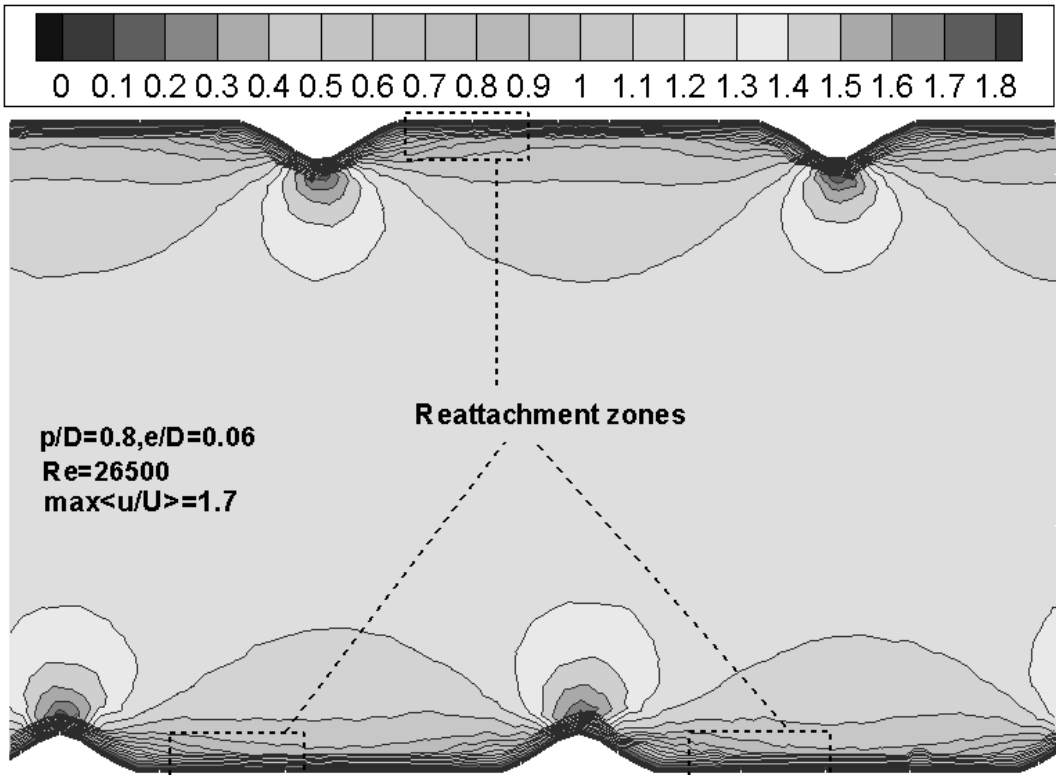

Fig.8: Dimensionless u-velocity contour and reattachment zones between ribs

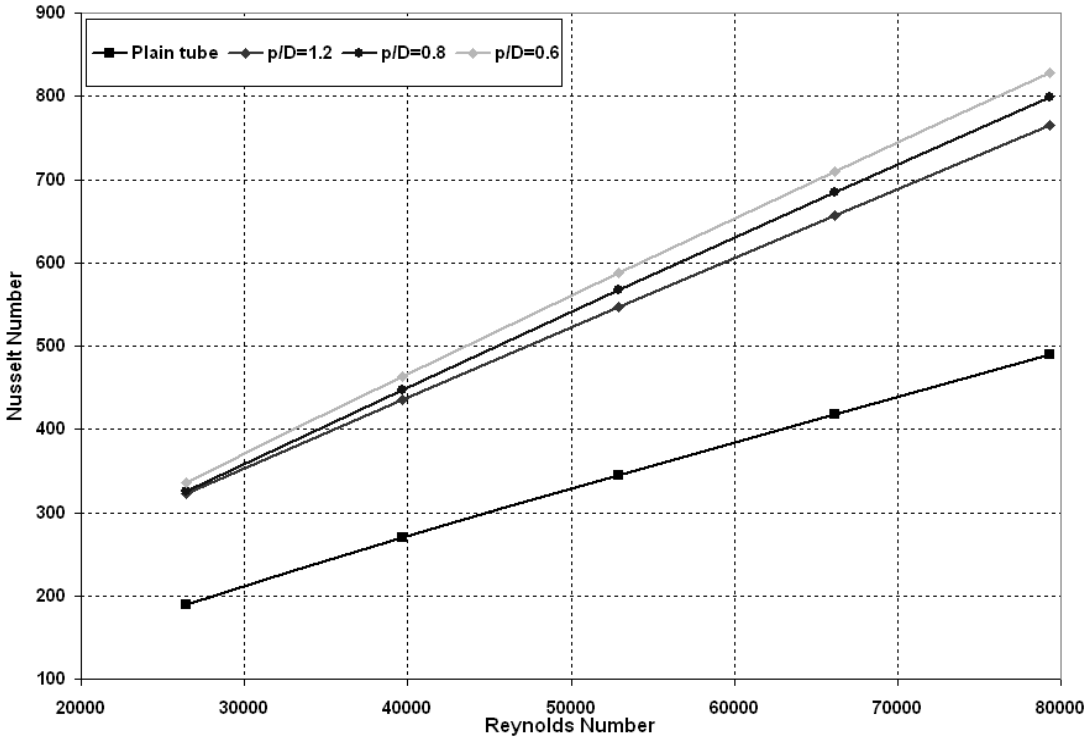

Fig.9: Variation of Nusselt number with Reynolds number for e/D=0.04

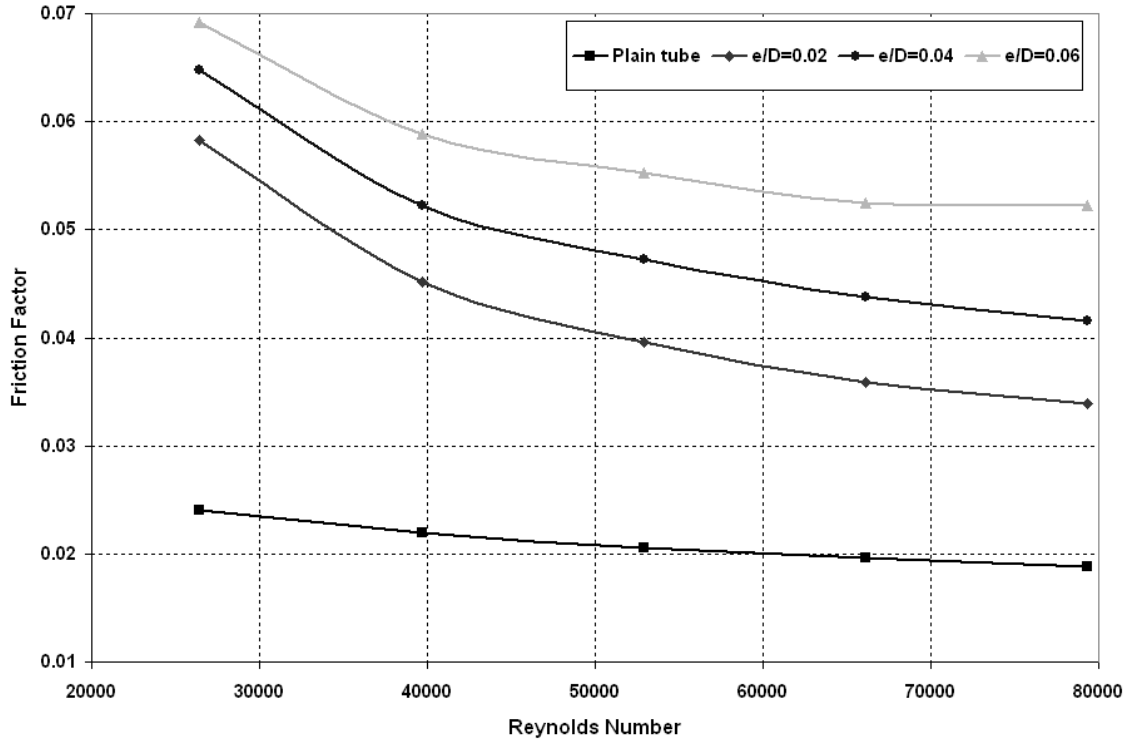

Fig.10: Variation of friction factor with Reynolds number for p/D=0.8

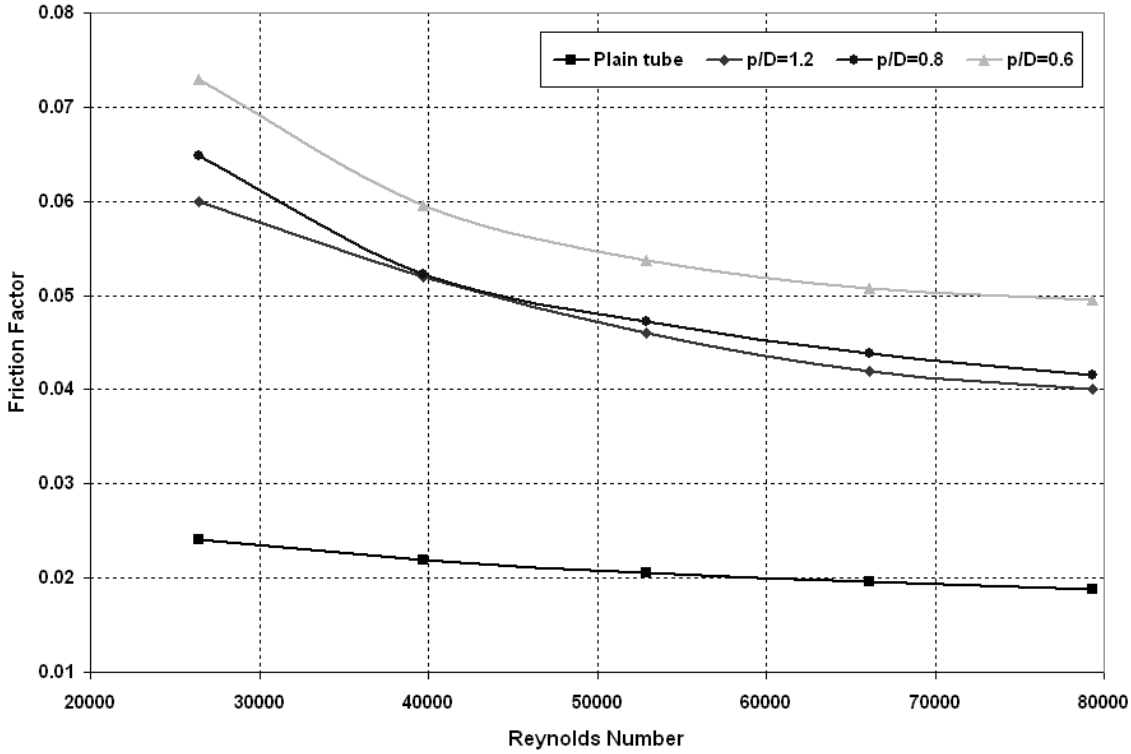

Fig.11: Variation of friction factor with Reynolds number for e/D=0.04